Improving the quality of compressed sensing MRI that exploits adjacent slice similarity

Norihito Inamuro and Akira Hirabayashi*
* College of Information Science and Engineering, Ritsumeikan University, Kusatsu, Japan
E-mail: akirahrb@media.ritsumei.ac.jp Tel: +81-77-507-0410

***Abstract*—We propose a fast magnetic resonance imaging (MRI) technique based on the method proposed by the present authors. The method exploited the combination of full and compressed sensing. Full sensing is taken at a set period (F-slice) while high compression rate sensing is applied to the rest of the slices (C- slice). If we set the F-slice every four slices, three C-slices are continuously located between two F-slices. We noticed a tendency, however, that the quality of the reconstructed image for the center C-slice is the lowest among the three C-slices. To solve this problem, we adjust the setup of the proposed method with regards to two aspects. First, we adjust compression rate. We reduce the sensing rate for the F-slices while increase the sensing rate for the C-slices. Second, we adjust the F-slice interval. When we set the F-slice at every two slices, the C-slice is always located between the F-slices and the distance of the F-slice and C-slice gets smaller. Thus, we can exploit more correct information to reconstruct C-slices. Simulation results show the effectiveness of the proposed method.**

I. Introduction

Magnetic Resonance Imaging (MRI) is now regarded as one of the indispensable medical modalities. The most significant issue of MRI is its long imaging time, which makes MRI's application areas very restrictive. To reduce the time, great efforts have been dedicated so far [1], [2]. Recently, the so-called compressed sensing is established and shown to be effective for a fast MRI. Compressed sensing is a technique that enables us to recover sparse or sparsely represented signals from linear measurements less than a signal dimension. Recovery is done by minimization of the number of nonzero entries or ℓ_1-norm under the observation constraint [3], [4], [5]. The framework of this theory perfectly matches and was successfully applied to MRI [6], [7]. Sparsity found in wavelet tree structure is also exploited in MR image reconstruction [8], [9]. These methods exploit sparsity only within each slice.

An MRI normally captures tens or hundred of slices with a distance of a few millimeters. Then, the neighboring slices are similar to each other. Such similarity was exploited in image reconstruction. Dictionary learning is one of such method [10]. It is, however, computationally expensive. To reduce the cost, the use of a graphics processing unit (GPU) was also proposed [11]. The present authors have exploited this similarity in a different way. Because of the similarity, it is possible to guess a slice from its neighbors. Further, the difference of the estimated image from the true image is small and sparse. Hence, we can reconstruct the difference precisely using the standard compressed sensing MRI technique. The present authors have implemented this idea by a combination of full and compressed sensing [12]. Full sensing is taken at a set period (F-slice), while compressed sensing with high compression rate is done for slices (C-slice) between the F-slices. Then, we can perfectly reconstruct F-slices, which are used to roughly estimate C-slice images. The estimate is called a reference image. The difference of the target image from the reference can be precisely estimated because it is small and sparse. This method performed better than not only the slice-by-slice method [6], [7], but also a method that exploits slice similarity. We noticed, however, through multiple simulations, a tendency of this method. For example, if we set the F-slice every four slices, then there are three C-slices continuously located between two F-slices. Two side C-slices are contiguous to the F-slices while the center C-slices are apart from them. As a results, the two side C-slices are reconstructed with a high quality while the quality of the reconstructed image for the center C-slice is not so high compared to those for the side C-slices. To solve this problem, we adjusted the setup of the proposed method with regards to two aspects. First, we adjust compression rate. We reduce the sensing rate for the F-slices while increase that for the C-slices. Second, we adjust the F-slice interval. When we set the F-slice at every two slices, C-slice is always located between the F-slices and distance of the F-slice and C-slice gets small. Thus, we can exploit more correct information to reconstruct C-slices.

The rest of the present paper is organized as follows. Section 2 formulates the problem of compressed sensing MRI and quickly reviews conventional approach. Section 3 summarizes the method proposed in [12] and show the tendency using simulation results. In Sections 4 and 5, we show that the performance of the proposed method can be further improved by adjusting the setup. Section 4 adjusts the compression rate for each slice while Section 5 controls the F-slice interval. Simulation results show the effectivness of these adjustments. Section 6 concludes the paper.

II. Compressed sensing MRI

To obtain slice images in a non-invasive manner, MRI applies appropriate magnetic fields to a human body and resonance signals are observed by sensors. The observed signal $\boldsymbol{y} \in \mathbb{R}^M$ is the two dimensional discrete Fourier transform of the slice image $\boldsymbol{x} \in \mathbb{R}^N$, as $\boldsymbol{y} = F\boldsymbol{x} + \boldsymbol{e}$, where F is the observation matrix, which is the two dimensional Fourier transform in the present case. The vector $\boldsymbol{e}$ is the observed noise. If enough observation, such as $M \geq N$, is available

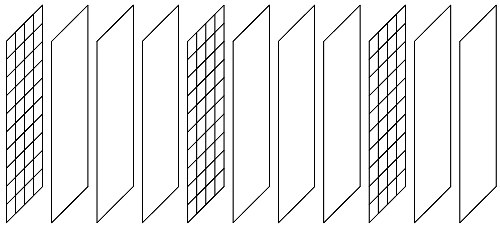

Fig. 1. Combination of full and compressed sensing. Full sensing is applied for the meshed slice (F-slice), while compressed sensing with high compression ratio is conducted for the rest of slices (C-slice).

and noise can be ignored, then the inverse discrete Fourier transform F^{-1} provides the slice image $\boldsymbol{x}$. The observation time for $\boldsymbol{y}$ is proportional to the number of measurements M. Hence, the less number of measurements we acquire, the shorter the observation time becomes. If we simply apply the inverse discrete Fourier transform to the reduced number of measurements, however, then artifacts like false edges or blur arise in the reconstructed image. Technology to solve this problem is compressed sensing [3], which guarantees that, when a target image is sparse or sparsely represented, it is perfectly reconstructed from measurements less than the image dimension. Compressed sensing exploits randomness in observation. In the present case, the Fourier coefficients are randomly selected. Let A be the random partial discrete Fourier transform. Then, the observation process is formulated as,

$$\boldsymbol{y} = A\boldsymbol{x} + \boldsymbol{e}, \tag{1}$$

From the random measurements, images are reconstructed by ℓ_1-norm minimization:

$$\boldsymbol{x}^{(1)} = \operatorname*{argmin}_{\boldsymbol{x}\in\mathbb{R}^N} \|\Psi\boldsymbol{x}\|_1 \text{ s.t. } \|A\boldsymbol{x}-\boldsymbol{y}\|_2 \le \varepsilon, \tag{2}$$

where ε bounds the amount of noise in the data. The sparsifying transform Ψ can be discrete wavelet transform, curvelet [13], or contourlet [14]. MR images further satisfy a prior knowledge that total-variation is small. Then, reconstruction images are obtained by solving the following problem:

$$\boldsymbol{x}^{(2)} = \operatorname*{argmin}_{\boldsymbol{x}\in\mathbb{R}^N} \|\Psi\boldsymbol{x}\|_1 + \alpha TV(\boldsymbol{x}) \text{ s.t. } \|A\boldsymbol{x}-\boldsymbol{y}\|_2 \le \varepsilon, \tag{3}$$

where α controls the balance between the Ψ-sparsity and the total variation. Similarly, a solution to the problem

$$\boldsymbol{x}^{(3)} = \operatorname*{argmin}_{\boldsymbol{x}\in\mathbb{R}^N} \|A\boldsymbol{x}-\boldsymbol{y}\|_2^2 + \lambda_1\|\Psi\boldsymbol{x}\|_1 + \lambda_2 TV(\boldsymbol{x}) \tag{4}$$

is also used for the MRI reconstruction. Here, λ_1 and λ_2 are regularization parameters.

III. Exploiting Neighboring Slice Similarity

A multislice MRI captures tens or hundred of slices with distance of a few millimeters. Then, neighboring slices are similar to each other. Thus, it is possible to guess a slice from its neighbors. Further, difference of the estimated image from the true image is small and sparse. Hence, we can reconstruct the difference precisely using the standard compressed sensing MRI technique [7]. The present authors have implemented this idea by a combination of full and compressed sensing [12]. Full sensing is taken at a set period (F-slice) while compressed sensing with high compression rate is applied to the rest of the slices (C-slice). Figure 1 explains a case where full sensing is taken every four slices, indicated by the meshed ones. We can perfectly reconstruct the F-slice images because of the full sensing. Then, these images are used to roughly estimate the neighboring C-slices. Since the estimate is already of good quality, its difference from the original image is small and sparse. Note that this sparsity is in the space domain, not in sparsified domain. Therefore, there is a possibility that, if we apply an appropriate sparsifying transform to this difference image, sparsity can be further promoted.

This idea mentioned above is formulated as follows. A reference image generated using neighboring F-slices is denoted by $\boldsymbol{x}_{ref}$. Then, the target slice $\boldsymbol{x}$ is expressed as a sum of the reference and difference, as $\boldsymbol{x} = \boldsymbol{x}_{ref} + \boldsymbol{d}$. Substituting this to (1) amounts to

$$\boldsymbol{y}_d = A\boldsymbol{d} + \boldsymbol{e}, \tag{5}$$

where $\boldsymbol{y}_d = \boldsymbol{y} - A\boldsymbol{x}_{ref}$, containing only given information. Since $\boldsymbol{d}$ is supposed to be sparse enough, it can be precisely reconstructed by the conventional techniques. Here, we adopt the problem (4), as

$$\hat{\boldsymbol{d}} = \operatorname*{argmin}_{\boldsymbol{d}\in\mathbb{R}^N} \|A\boldsymbol{d}-\boldsymbol{y}_d\|_2^2 + \lambda_1\|\Psi\boldsymbol{d}\|_1 + \lambda_2 TV(\boldsymbol{d}). \tag{6}$$

Now the problem is converted to the problem of estimating the difference $\boldsymbol{d}$ given its observation model (5). The final results is then obtained by the sum of $\hat{\boldsymbol{d}}$ and $\boldsymbol{x}_{ref}$, as $\hat{\boldsymbol{x}} = \boldsymbol{x}_{ref} + \hat{\boldsymbol{d}}$.

We show simulation results by the method in [12]. The data used in this simulation were acquired at Ritsumeikan University in 2014 with two male healthy patients, say A and B, of twenty years old using GE 1.5T MRI scanner. This data set contains 256 x 256 images in the Dicom format. The pixel resolution is 0.5 mm and the slice distance is 1 mm. The brain and right arm parts were scanned for the patients A and B, and 154 and 54 images were obtained, respectively. Among them, five continuous image sequences were extracted and used in the following simulations. Programs are run using Matlab R2013b on iMac with 2.4GHz Intel Core i5 processor and 8 GB memory.

Figure 2 shows the results obtained by the method. Images 1 and 5 are the F-slices and the rest are C-slices with compression rate 1/9. F-slices are perfectly reconstructed. Three C-slices are reconstructed with a high quality. We found that, however, the center C-slices are reconstructed with the lowest quality among the C-slices. The main reason of this is because the center C-slice is the furthest from the neighboring F-slices and hence the quality of its reference image degrades. Solving this problem can further improve the performance of the proposed method. Hence, in this paper, we adjust the setup of the proposed method in the sense of two aspects.

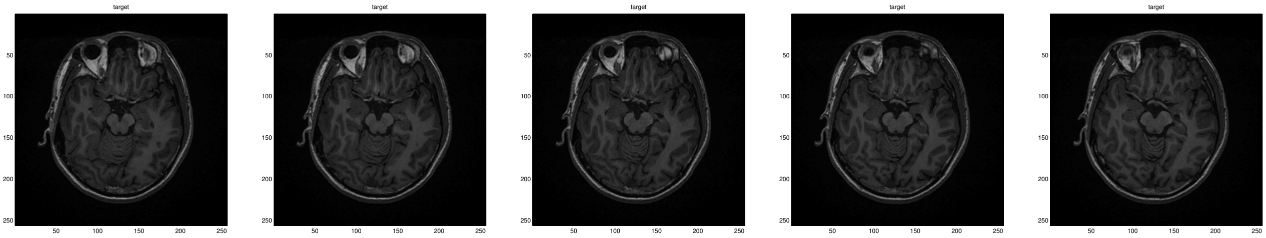

#1 #2 #3 #4 #5

(a) Target brain images of 1mm slice

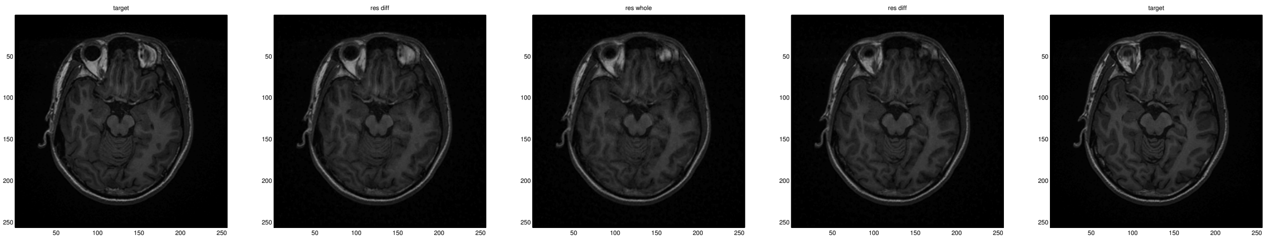

Perfect reconst. 38.63dB (1/9) 37.55dB (1/9) 39.14dB (1/9) Perfect reconst.

(b) Results obtained by the method in [12]

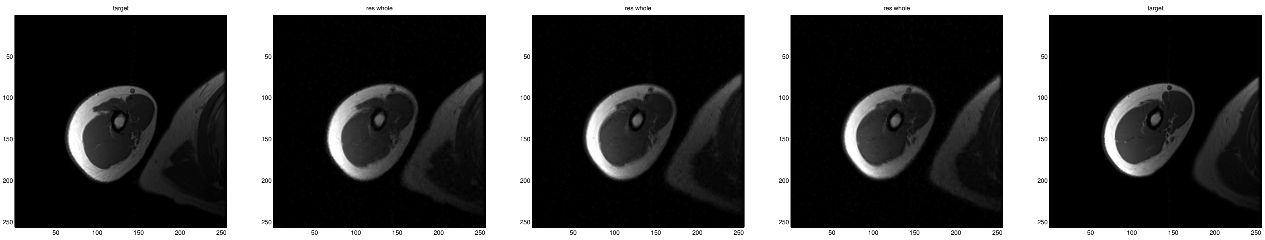

#1 #2 #3 #4 #5

(c) Target arm images of 1mm slice

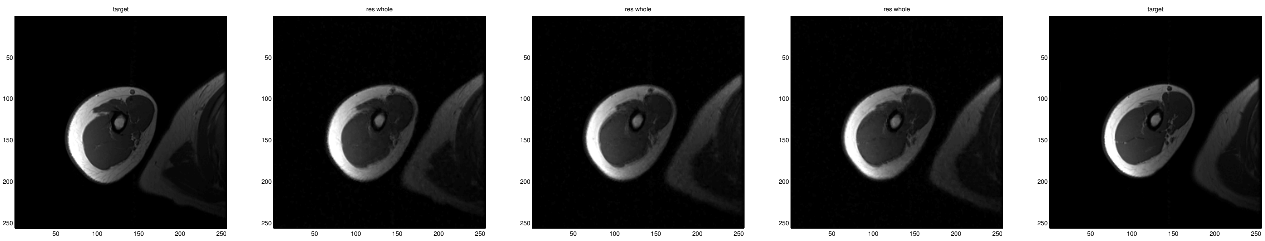

Perfect reconst. 39.14dB (1/9) 38.94dB (1/9) 38.53dB (1/9) Perfect reconst.

(d) Results obtained by the method in [12]

Fig. 2. Target image and results obtained by the method in [12]

One is the compression rate, the other is the interval of the F-slices. The former is discussed in Section IV while the latter will be discussed in Section V.

IV. Modifying compression rate

In this section, we improve the performance of the proposed method by adjusting the compression rate for the F- and C-slices. We reduce the sensing rate for the F-slices while increase that for the C-slices with maintaining the total sensing rate the same. Since the F-slice is no longer fully sampled, we call the modified F- and C-slices I- and D-slices, respectively. The I-slice stands for an Independent slice and it will be reconstructed independently from other slices as well as the F-slices. The D-slice stands for a Dependent slice, which is reconstructed using the neighboring two I-slices.

The I-slices are taken every four slices. Three slices between them are the D-slices. We adopted the compression rate 1/2 for the I-slices. This means that the compression rate for the D-slice becomes 5/18 to keep the average compression rate 1/3.

Figures 3 (a) and (c) show simulation results. Even though I-slices are not fully sampled, the compression rate is not so severe. Hence, we can reconstruct the slice with high quality using the standard compressed sensing MRI technique [6]. Indeed, images 1 and 5 (I-slices) are reconstructed with high PSNRs more than 40dB. The rest are D-slices. The reference images for D-slices were generated by the linear interpolation of the reconstructed images for images 1 and 5. PSNRs of the three D-slices are more than 1dB higher than those in Figure

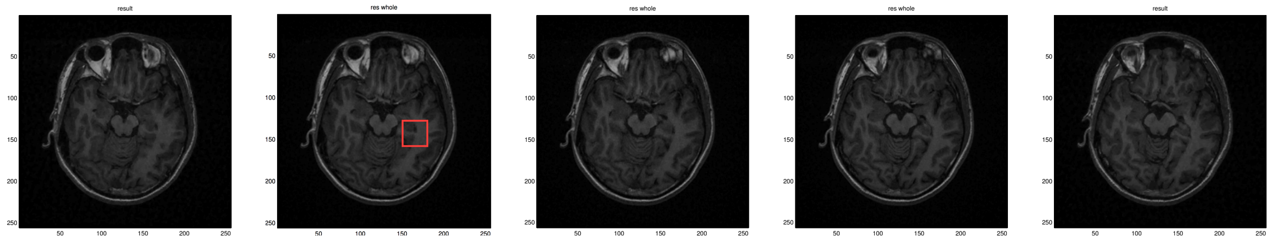

44.85dB (1/2) 39.71dB (5/18) 39.33dB (5/18) 40.13dB (5/18) 45.17dB (1/2)

(a) Results obtained after compression rate modification

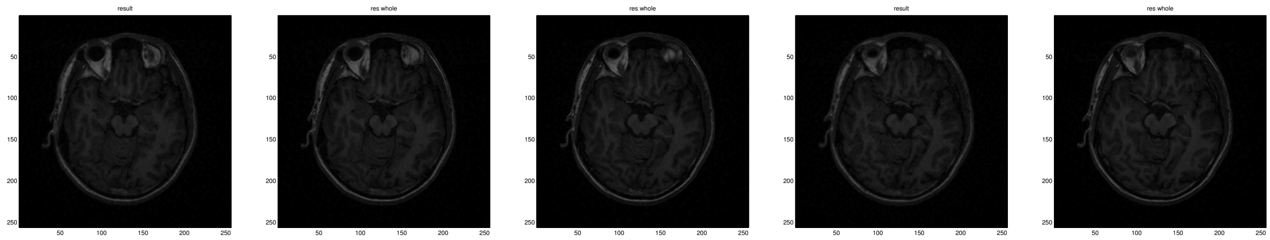

44.85dB (1/2) 37.97dB (1/4) 38.34dB (1/4) 45.10dB (1/2) 38.82dB (1/4)

(b) Results obtained by Pang et al. [15]

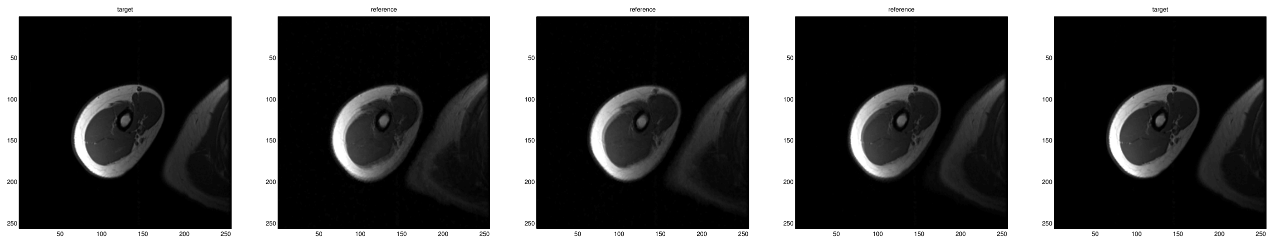

56.58dB (1/2) 45.03dB (5/18) 42.84dB (5/18) 43.00dB (5/18) 57.17dB (1/2)

(c) Results obtained after compression rate modification

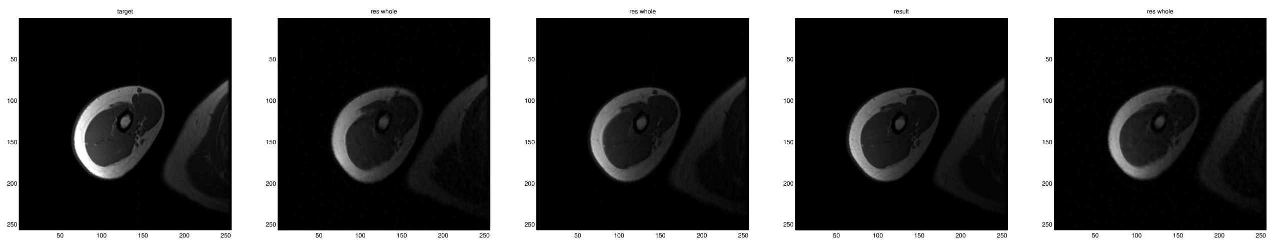

56.58dB (1/2) 36.48dB (1/4) 39.26dB (1/4) 57.22dB (1/2) 35.45dB (1/4)

(d) Results obtained by Pang et al. [15]

Fig. 3. Results obtained by proposed method and Pang et al. [15]

2. The averages of PSNRs for the brain and arm images 1 $\sim$ 5 are 42.50dB and 49.12dB, respectively. Figures 3 (b) and (d) show the results by the method of Pang et al [15]. It reconstructs images 1 and 4 independently, which we shall call I-slices. It also reconstructs images 2, 3, and 5 by referring the adjacent I-slices, which we shall call D-slice. We used the compression rate 1/2 for the I-slices and 1/4 for the D-slice. The average of PSNRs for brain and arm image 1 $\sim$ 5 are 40.57dB and 44.99dB, respectively. That is, our approach results in higher reconstruction quality than the conventional method. The boxed area is zoomed in Figure 4, in which (a), (b), and (c) show the target image, result obtained by the proposed method, and that obtained by the method of Pang et al. [15], respectively. The image in (c) is rougher than that in (b). The boundary in the image center in (b) is clearer than that in (c).

V. Modifying I-slice interval

By reducing the sensing amount for the I-slices and aquiring more measurements for the D-slices, the quality of the reconstructed images were improved, as is shown in the previous section. Unfortunately, we still see the tendency that the center slice is of the lowest quality among the D-slices. Hence, in

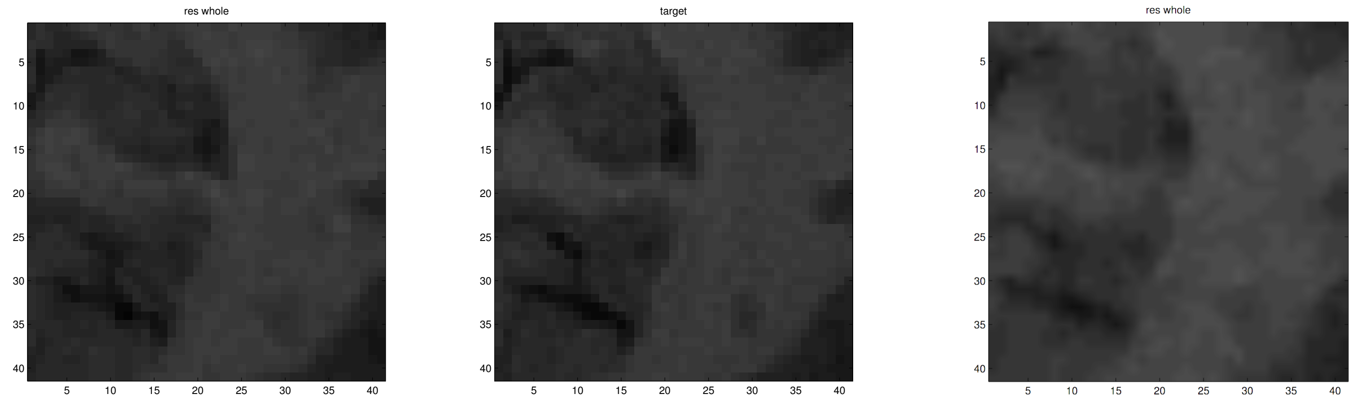

(a) Target image (b) Results obtained by the proposed method (c) Results obtained by Pang et al. [15]

Fig. 4. The zoomed images of the circled area in Figure3

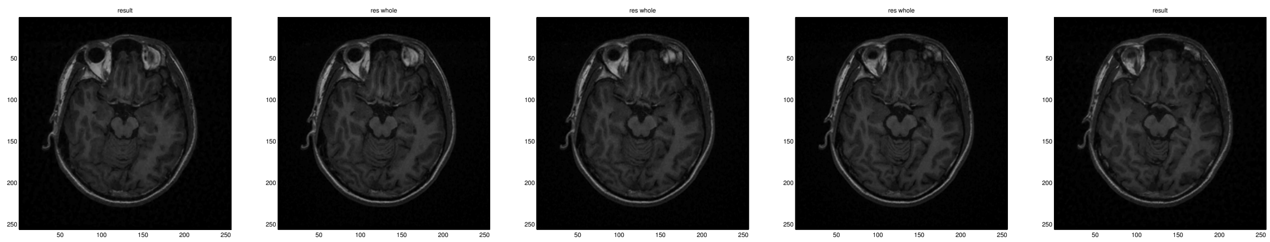

44.85dB (1/2) 39.80dB (1/6) 45.33dB (1/2) 40.01dB (1/6) 45.17dB (1/2)

(a) Results obtained for the brain images

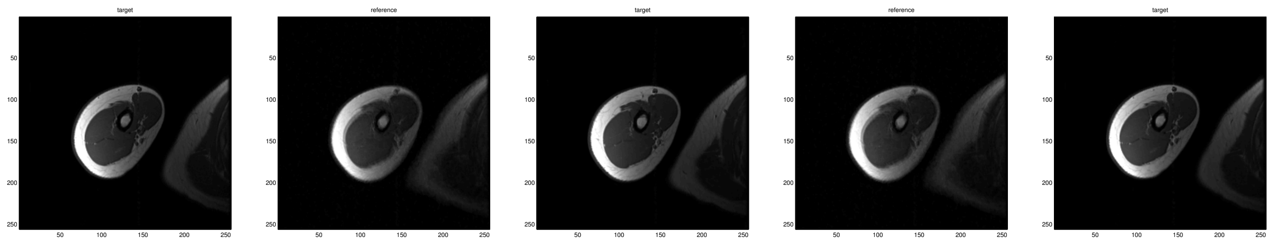

56.58dB (1/2) 42.89dB (1/6) 55.85dB (1/2) 40.67dB (1/6) 57.17dB (1/2)

(b) Results obtained for the Arm images

Fig. 5. Results obtained with I-slice every two slices I-slice interval

this section, we reduce the I-slice interval to avoid the center D-slice problem. That is, we set the I-slice at every two slices. Each D-slice lies between I-slices adjacently. Since distance of the I-slices and D-slice is reduced, we can produce a high quality reference image.

Figure 5 shows simulation results. We adopted the compression rate 1/2 for the I-slices. This means that the compression rate for the D-slice becomes 1/6 to keep the average compression rate 1/3. The average of PSNRs for the brain images 1 $\sim$ 5 is 43.03dB and that for the arm images 1 $\sim$ 5 is 50.63dB. Hence, the average of PSNRs is better than that in the previous section even though the PSNR for the arm image 2 got worse.

VI. Conclusion

In the method proposed by the authors in [12], there was a tendency that the center C-slice shows the lowest quality. To solve this problem, we adjusted the setup of the proposed method with regards to two aspects. One is the compression rate. We reduced the sensing rate for the F-slice and increased that for the C-slice. In this context, we referred the F- and C-slices as the I- and D-slices. The other is the interval of the I-slices. We obtained the I-slice every two slices. Since the quality of the reference image is higher than that before the reduction of the I-slice interval, the quality of the reconstructed images became higher and more uniform. One direction to further improve the performance of the proposed method is to produce better reference images. To this end, to exploit anatomical information is one of our future tasks.

Ackonwedgment

This research was partially supported by the Research Grant from the Kayamori Foundation of Informational Science Advancement. The authors are grateful to Prof. Jeremy White in Ritsumeikan University for improving English expressions. We thank Dr. Kurihara and Dr. Homma for providing the MR images.

References

[1] D.K. Sodickson and W.J. Manning, "Simultaneous acquisition of spatial harmonics (SMASH): fast imaging with radiofrequency coil arrays," *Magnetic Resonance in Medicine*, vol. 38, no. 4, pp. 591–603, 1997.

[2] K.P. Pruessmann, M. Weiger, M.B. Scheidegger, and P. Boesiger, "SENSE: sensitivity encoding for fast MRI," *Magnetic Resonance in Medicine*, vol. 42, no. 5, pp. 952–962, 1999.

[3] D.L. Donoho, "Compressed sensing," *IEEE Transactions on Information Theory*, vol. 52, no. 4, pp. 1289 –1306, april 2006.

[4] E.J. Candes and M.B. Wakin, "An introduction to compressive sampling," *IEEE Signal Processing Magazine*, vol. 25, no. 2, pp. 21–30, March 2008.

[5] Y.C. Eldar and G. Kutyniok, *Compressed Sensing: Theory and Applications*, Cambridge University Press, Cambridge, 2011.

[6] M. Lustig, D. Donoho, and J.M. Pauly, "Sparse MRI: The application of compressed sensing for rapid MR imaging," *Magnetic Resonance in Medicine*, vol. 58, pp. 1182–1195, 2007.

[7] M. Lustig, D.L. Donoho, J.M. Santos, and J.M. Pauly, "Compressed sensing MRI," *IEEE Signal Processing Magazine*, vol. 25, no. 2, pp. 72–82, 2008.

[8] C. Chen and J. Huang, "Compressive sensing MRI with wavelet tree sparsity," in *Advances in Neural Information Processing Systems 25*, P. Bartlett, F.C.N. Pereira, C.J.C. Burges, L. Bottou, and K.Q. Weinberger, Eds., pp. 1124–1132. Curran Associates Inc., 2012.

[9] Z. Zhu, K Wahid, P. Babyn, and R. Yang, "Compressed sensing-based MRI reconstruction using complex double-density dual-tree DWT," *Journal of Biomedial Imaging*, vol. 2013, no. 10, pp. 12, 2013.

[10] Y. Song, Z. Zhu, Y. Lu, Q. Liu, and J. Zhao, "Reconstruction of magnetic resonance imaging by three-dimensional dual-dictionary learning," *Magnetic Resonance in Medicine*, vol. 71, pp. 1285–1298, 2014.

[11] J. Li, J. Sun, Y. Song, Y. Xu, and J. Zhao, "Accelerating the reconstruction of magnetic resonance imaging by three-dimensional dual-dictionary learning using cuda," in *36th Annual International Conference of the IEEE Engineering in Medicine and Biology Society (EMBC)*, 2014, pp. 2412–2415.

[12] Akira Hirabayashi, Norihito Inamuro, K. Mimura, T.Kurihara, and T.Homma, "Compressed sensing mri using sparsity induced from adjacent slice similarity," in *Proceedings of 11th International Conference on Sampling Theory and Applications (SampTA 2011)*, Washington D.C., 2015, pp. 5 pages (CD–ROM), (CD-ROM).

[13] M.N.Do and M. Vetterli, "The contourlet transform: An efficient directional multiresolution image representation," *IEEE Transactions on Image Processing*, vol. 14, no. 12, pp. 2091–2106, Dec. 2005.

[14] E.J. Candes and D.L. Donoho, "New tight frames of curvelets and optimal representations of objects with piecewise c^2 sigularities," *Communications on Pure and Applied Mathematics*, vol. 57, no. 2, pp. 219–266, Feb. 2004.

[15] Yong Pang and Xiaoliang Zhang, "Interpolated compressed sensing for 2D multiple slice fast MR imaging," *PLoS ONE*, vol. 8, no. 2, pp. e56098, 02 2013.